



Creep-fatigue life evaluation of high chromium ferritic steel under non-proportional loading

T. Morishita, Y. Murakami

Graduate School of Science and Engineering, Ritsumeikan University, Japan
gr0202xp@ed.ritsumei.ac.jp, rm0038kk@ed.ritsumei.ac.jp

T. Itoh

College of Science and Engineering, Ritsumeikan University, Japan
itohtaka@fc.ritsumei.ac.jp

H. Tanigawa

National Institutes for Quantum and Radiological Science and Technology, Japan
tanigawa.hiroyasu@qst.go.jp

ABSTRACT. T Multiaxial creep-fatigue tests under non-proportional loading conditions with various strain rates were carried out using a hollow cylinder specimen of a high chromium ferritic steel at 823K in air to discuss the influence of non-proportional loading on failure life. Strain paths employed were a push-pull loading and a circle loading. The push-pull loading test is proportional strain path test. The circle loading test is non-proportional strain path test in which sinusoidal waveforms of axial and shear strains have 90 degree phase difference. The failure life is affected largely by the strain rate and the non-proportional loading. This paper presents a modified strain range for life evaluation considering the strain rate based on a non-proportional strain parameter proposed by authors. The strain range is a suitable parameter for life evaluation of tested material under non-proportional loading at high temperature.

KEYWORDS. Life evaluation; Creep-fatigue; Multiaxial strain; Non-proportional loading; High chromium ferritic steel.



Citation: Morishita, T., Murakami, Y., Itoh, T., Tanigawa, H., Creep-fatigue life evaluation of high chromium ferritic steel under non-proportional loading, *Frattura ed Integrità Strutturale*, 38 (2016) 281-288.

Received: 30.07.2016

Accepted: 31.08.2016

Published: 01.10.2016

Copyright: © 2016 This is an open access article under the terms of the CC-BY 4.0, which permits unrestricted use, distribution, and reproduction in any medium, provided the original author and source are credited.

INTRODUCTION

In the blanket structure of a demonstration fusion reactor, the material receives severe cyclic loading conditions such as combined thermal and mechanical cyclic deformations. By the combination of thermal and mechanical loading, the non-proportional loading in which the principal stress and strain directions rotate in a cycle occurs. It has been

reported that failure lives are reduced accompanying with an additional hardening due to non-proportional loading depending on both the strain path and the material [1-5]. The failure life under non-proportional loading at high temperature has been discussed in the previous study for the high chromium ferritic steel [6]. However, open questions of discussing creep-fatigue property still exist. Therefore, creep-fatigue test results and damage evaluation under multiaxial loading are required for reliable and safety design of strength for materials and components.

In this study, creep-fatigue tests under a push-pull loading and a circle loading conditions with changing the strain rate were performed at 823K in air. The evaluation of failure life is also discussed from the obtained test results.

EXPERIMENTAL PROCEDURE

Multiaxial creep-fatigue tests under non-proportional loading with various waveforms were carried out at 823K in air. A hollow cylinder specimen which has a 9mm inner-diameter, a 12mm outer-diameter and a 12mm in a gauge length as shown in Fig. 1 was employed. The testing machine used was an electrical servo hydraulic tension and torsion fatigue testing machine. Strain paths and strain waveforms are shown in Fig. 2. They are the push-pull loading (PP) and the circle loading (CI). The PP test is the proportional strain loading test. The CI test is the non-proportional strain loading test in which axial strain and shear strain have 90 degree sinusoidal out-of-phase. Total axial strain and total shear strain ranges were the same ranges based on von Mises basis ($\Delta\epsilon = \Delta\gamma/\sqrt{3}$). In these strain paths, three strain rates were employed. They are 0.2%/s, 0.01%/s and 0.002%/s based on von Mises basis which are indicated by 'FF', 'SS' and 'SS*', respectively. Strain holdings are also employed, they are the tensile and the compressive holdings which are indicated by 'TH' and 'CH'. The holding times used were 180s (3min.) and 600s (10min.). Number of cycles to failure (failure life) N_f is defined as the cycles at which the axial or shear stress was reduced to 3/4 of the sudden decrease point.

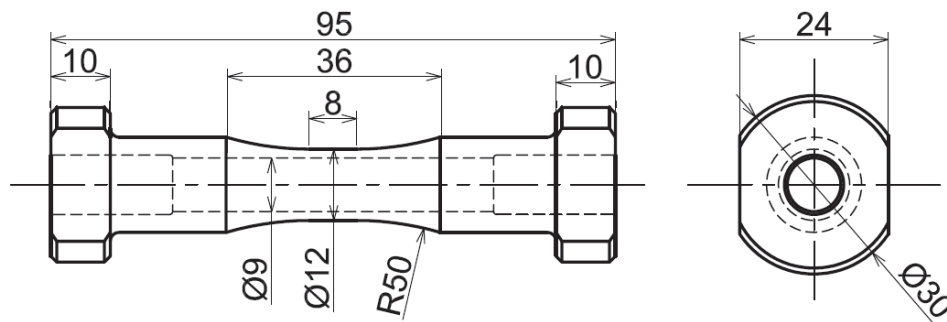


Figure 1: Shape and dimensions of test specimen (mm).

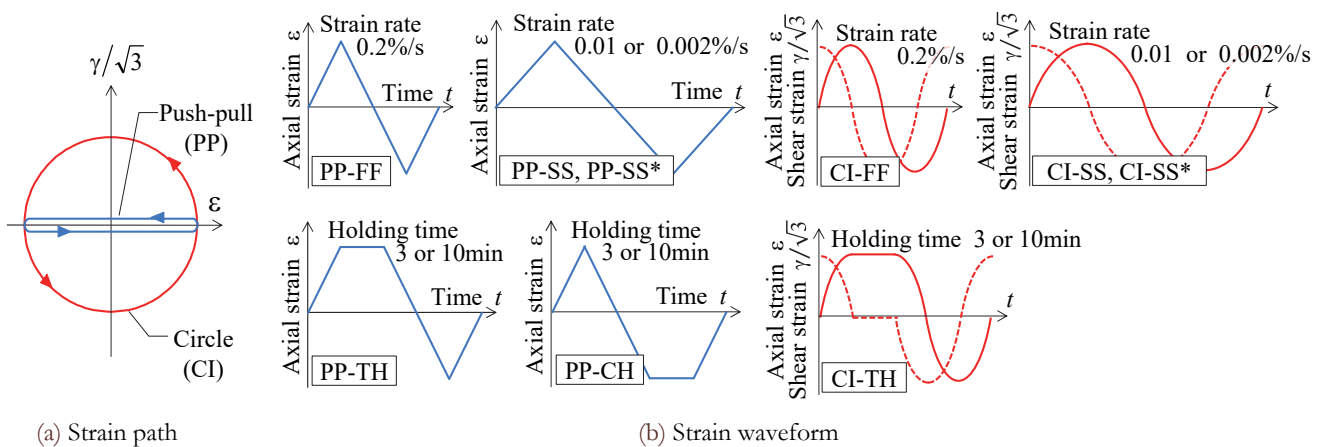


Figure 2: Strain path and strain waveform.

EXPERIMENTAL RESULTS AND DISCUSSION

Failure Life

Tab. 1 and Fig. 3 show the test results and the failure life. The failure life is affected largely by not only strain path (strain non-proportionality) but also strain waveform (creep damage). In the PP test, the failure life is reduced with the decrease in the strain rate under the same strain range, which may be resulting from larger creep damage caused by the lower strain rate. On the other hand, in the CI test, the failure life is increased when the strain rate is reduced from 0.2%/s to 0.01%/s, but the failure life is decreased by the further reduction in the strain rate from 0.01%/s to 0.002%/s. The former may be resulting from the reduction in the intensity of strain non-proportionality caused by stress relaxation due to creep and the latter can be by the increase of creep damage.

Strain path	Waveform	Strain rate (%/s)	Holding time (s)	$\Delta \epsilon_{eq}$ (%)	N_f (cycles)	
Push-pull	PP-FF	0.2	0	0.5	2,757	
				1.0	680	
	PP-SS	0.01		0.5	1,980	
				1.0	501	
	PP-SS*	0.002		0.5	1,780	
				0.7	945	
			1.0	323		
	PP-TH	0.2	180	0.5	2,389	
			180	1.0	543	
	600		600	0.5	2,442	
			600	1.0	523	
	PP-CH		180	0.5	1,718	
180			1.0	598		
Circle	CI-FF	0.2	0	0.5	870	
				1.0	240	
	CI-SS	0.01		0.5	1,452	
				1.0	378	
	CI-SS*	0.002		0.5	682	
				0.7	325	
			1.0	164		
	CI-TH	0.2	180	0.5	1,680	
			180	1.0	268	
			600	600	0.5	1,190
				600	1.0	302

Table 1: Test conditions and results.

Fig. 4 shows a correlation of the failure life by von Mises' equivalent strain range $\Delta\epsilon_{eq}$. In the figure, a bold solid line is drawn based on the data in the PP-FF test which is the life curve for life evaluation and two thin lines show a factor of 2 band. The bold solid line is given by

$$\Delta\epsilon_{eq} = AN_f^{-0.12} + BN_f^{-0.6} \quad (1)$$

where the coefficients A and B are defined as $3.5\sigma_B/E$ and $\epsilon_f^{0.6}$ according to the definition of the universal slope method [7]. In this study, B is put as the curve to be fit with the data in the PP-FF test. This figure shows clearly a large reduction in the failure life in the CI test compared with the PP test according to the non-proportional loading effect.

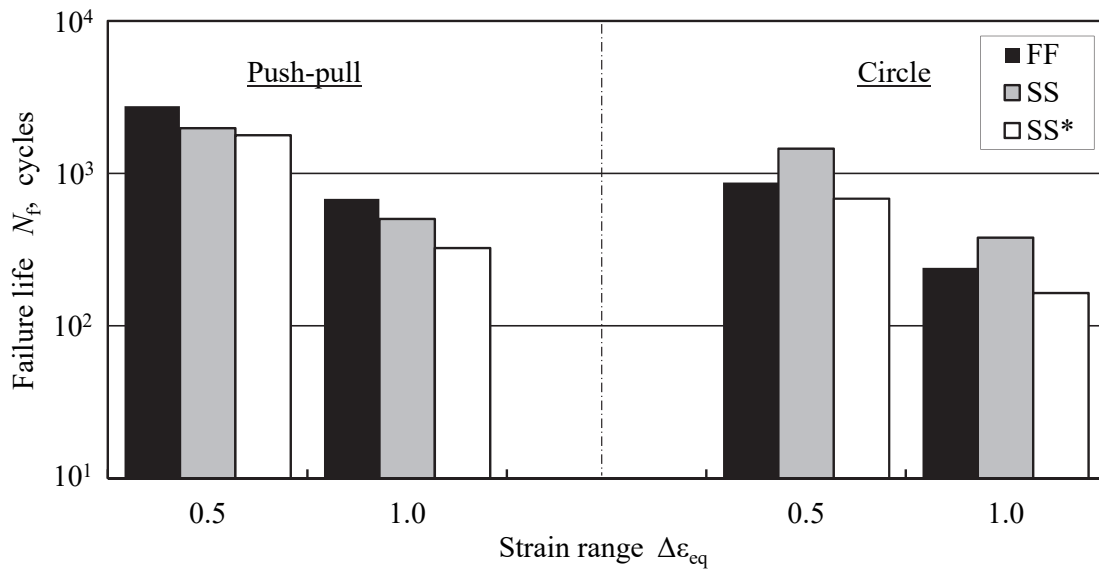


Figure 3: Comparison of creep-fatigue failure lives.

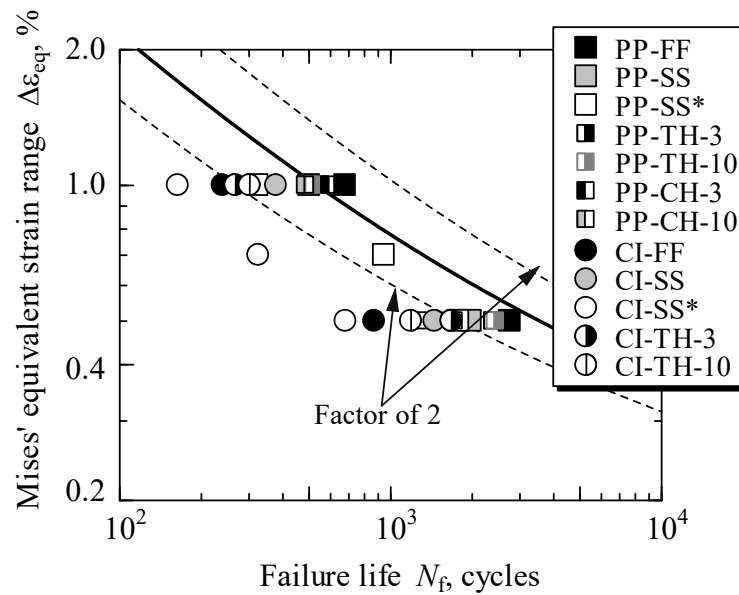


Figure 4: Correlation of N_f by Mises' equivalent strain range.

In multiaxial low cycle fatigue tests, it has been reported that the large reduction in the failure life has a close relation with strain path and material. Itoh *et al.* [8-13] proposed a non-proportional strain range $\Delta\epsilon_{NP}$ for life evaluation under non-proportional loading defined by

$$\Delta\epsilon_{NP} = (1 + \alpha f_{NP}) \Delta\epsilon_I \quad (2)$$

where $\Delta\epsilon_I$ is a maximum principal strain range under non-proportional loading which can be calculated by ϵ and γ . α and f_{NP} are a material constant and a non-proportional factor, respectively. The former is the parameter related to the additional hardening due to non-proportional loading and the latter is the parameter expressing the intensity of non-proportional loading. The value of α is the ratio to fit the failure life in the CI test to that in the PP test at the same $\Delta\epsilon_I$. f_{NP} is defined by [12]

$$f_{NP} = \frac{\pi}{2 S_{I\max} L_{\text{path}}} \int_C |\mathbf{e}_I \times \mathbf{e}_R| S_I(t) ds, \quad L_{\text{path}} = \int_C ds \quad (3)$$

where $S_I(t)$ is the maximum absolute value of principal strains at time t , $S_{I\max}$ is the maximum value of $S_I(t)$. \mathbf{e}_I and \mathbf{e}_R are unit vectors of $S_{I\max}$ and $S_I(t)$, ds the infinitesimal trajectory of the loading path. L_{path} is the whole loading path length during a cycle and “ \times ” denotes vector product. Integrating the product of amplitude and principal direction change of stress and strain by path length in Eq. (3) is a suitable parameter for evaluation of the additional damage due to non-proportional loading. Detail descriptions of f_{NP} and the life evaluations have been mentioned in reference [12] and are omitted here. f_{NP} in the PP test (proportional loading) takes 0 and that in the CI (non-proportional loading) takes 1.

Fig. 5 shows a correlation of the failure life by $\Delta\epsilon_{NP}$. This figure shows that dark symbols for PP-FF and CI-FF tests are plotted beside the bold line and $\Delta\epsilon_{NP}$ can evaluate non-proportional loading tests at the high strain rate. Because of creep damage, the failure lives in lower strain rates are scattered even though almost of all data are correlated within the factor of 2 band. Therefore, $\Delta\epsilon_{NP}$ may need some modification which considers the effect of strain rate.

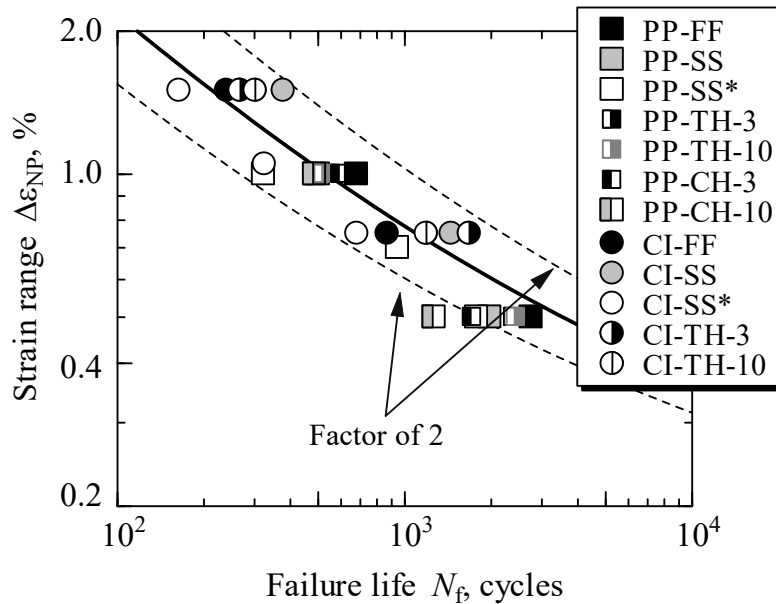


Figure 5: Correlation of N_f by non-proportional strain range.

Creep Fatigue Damage under Proportional Loading Condition

The evaluation method proposed by Coffin [14], which takes into account the strain rate under proportional loading, is employed for life evaluation. The equation is given by

$$\Delta\epsilon_p \left(\nu^{k-1} N_f \right)^\beta = C \quad (4)$$

where $\Delta\epsilon_p$ and ν are plastic strain and cyclic frequency. C , β and k are material constants. From the experimental results in PP-FF and PP-SS tests, the material constants and a correlation of strain ranges in PP-FF and PP-SS tests can be calculated by Eq. (5).

$$\Delta\epsilon_p^{\text{PP-FF}} = \Delta\epsilon_p^{\text{PP-SS}} \left(\frac{\nu}{\nu_0} \right)^{(k-1)\beta} \quad (5)$$

In this material at the tested temperature, k and β take 0.6 and 0.9, respectively. $\Delta\epsilon_{PP-FF}$ and $\Delta\epsilon_{PP-SS}$ are plastic strain ranges when N_f in PP-FF test takes the same value as that of PP-SS test. According to that correlation in this figure, a modified strain range $\Delta\epsilon_{NP}'$ can be defined as,

$$\Delta\epsilon_{NP}' = (1 + \alpha f_{NP}) K_v \Delta\epsilon_I, \quad K_v = \left(\frac{v}{v_0} \right)^{(k-1)\beta} \quad (6)$$

where v_0 is the frequency at the strain rate of the fatigue test in which creep effect can be ignored. In this study, the strain rate in the PP-FF test is set as v_0 . v is an arbitrary frequency in the tests with the lower strain rate of which creep effect is included. PP-TH, PP-CH and CI-TH tests which have strain holding are assumed to be transformed proximately into the test of triangular or sinusoidal waveform with low strain rate. Fig. 6 shows how to transform the strain waveform in the holding test into an equivalent strain waveform to obtain the strain rate v' . The strain rate is calculated from the equivalent strain waveform. Fig. 7 shows a correlation of the failure life by $\Delta\epsilon_{NP}'$. The data in PP test under various strain rates including strain holding is correlated within the factor of 2 band even though data in high strain ranged tests are plotted conservatively. On the other hand, the data in CI test under low strain rates is underestimated.

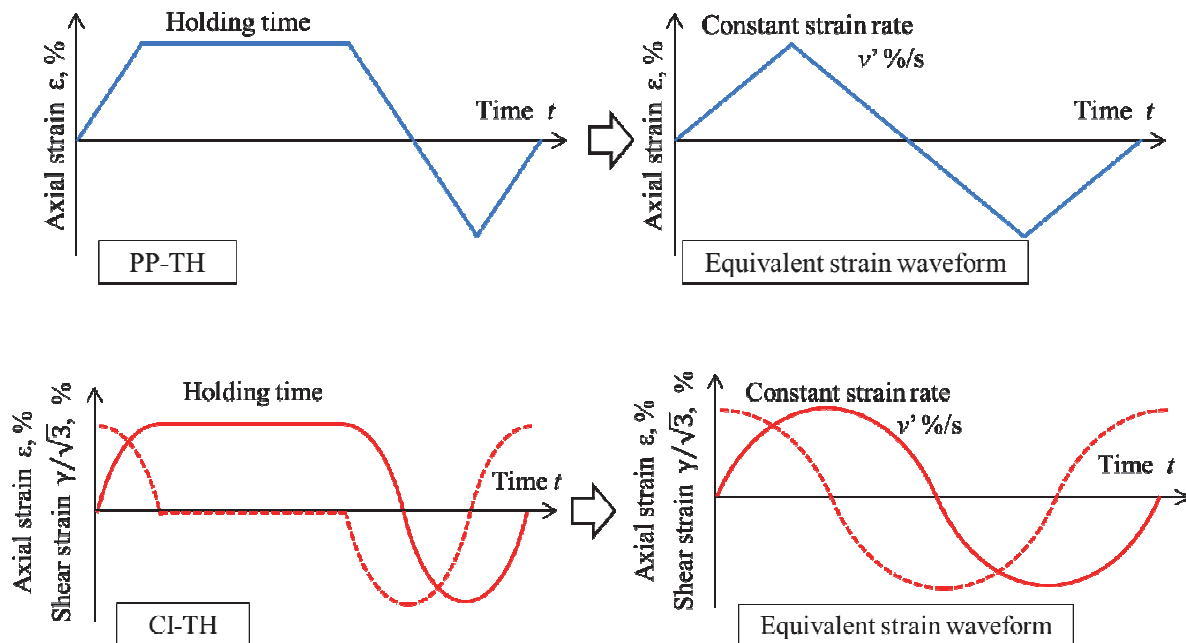


Figure 6: Assuming waveform of hold loading equivalent to triangular loading.

Creep Fatigue Damage under Non-proportional Loading Condition

The low strain rate reduces the failure life by creep damage. On the other hand, the intensity of strain non-proportionality decreases due to the stress relaxation caused by creep. For the life evaluation in low strain rates under non-proportional loading, a modified non-proportional strain range is proposed by Eq. (6) by adding a new parameter K_s which shows the reduction of intensity of non-proportionality. The modified strain range is given by

$$\Delta\epsilon_{NP}^* = (1 + \alpha K_s f_{NP}) K_v \Delta\epsilon_I \quad K_s = \chi \left(\frac{v}{v_0} - 1 \right) \quad (7)$$

where the value of K_s is calculated from test results in CI test, that is, a correlation of K_s with strain rate is obtained by data fitting. χ is a material constant, in case of this material $\chi=2.7$.

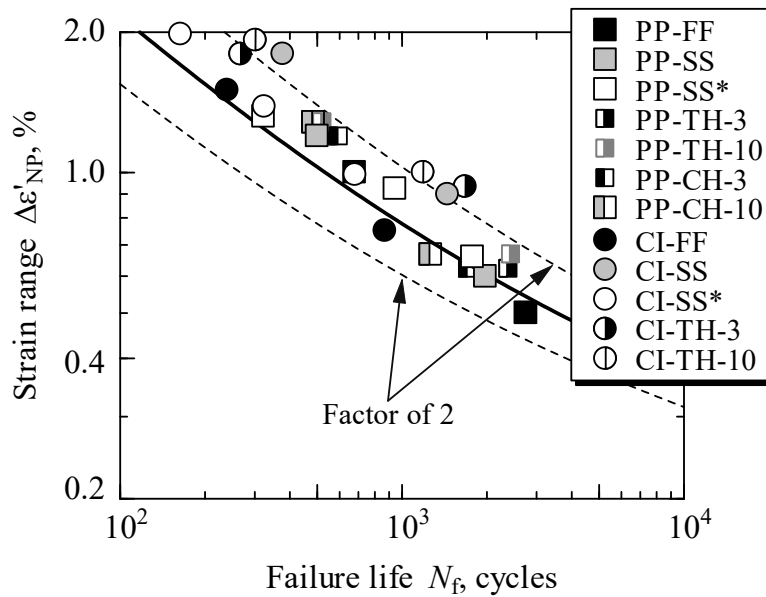


Figure 7: Correlation of N_f by modified non-proportional strain range.

Fig. 8 shows a correlation of failure life by the modified non-proportional strain range. In the figure, all of the data can be plotted within the factor of 2 band. It suggests that $\Delta\epsilon^*_{NP}$ becomes a suitable parameter for evaluation of the creep-fatigue failure life under non-proportional loading.

Further creep-fatigue tests using other materials will be obtained for the discussion of this modified non-proportional strain range considering the strain rate.

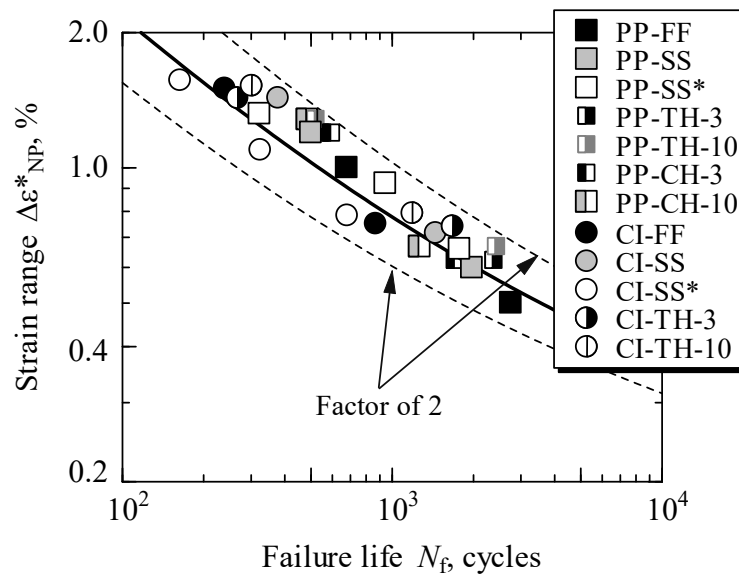


Figure 8: Correlation of N_f by modified non-proportional strain range.

CONCLUSIONS

- (1) In the push-pull loading test (proportional loading test), failure life is decreased with decreasing in the strain rate resulting in creep damage.

- (2) In the circle loading test (non-proportional loading test), failure life depends on the strain rate. The increase in the failure life can be explained by the reduction in the intensity of strain non-proportionality caused by stress relaxation due to creep. Conversely, the decrease in the failure life can be explained by the increase of creep damage.
- (3) The modified non-proportional strain range considering the strain rate can correlate the failure life very well.

ACKNOWLEDGEMENT

This work was supported by the Japan Atomic Energy Agency under the Joint Work contract #27K400, as a part of the work assigned to the Japanese Implementing Agency under the Procurement Number IFERC-T3PA4-JA-RP-1b within the "Broader Approach Agreement" between the Government of Japan and the European Atomic Energy Community.

REFERECES

- [1] Doong, S.H., Socie, D.F., Robertson, I.M., Dislocation substructures and nonproportional hardening, *Journal of Engineering Materials and Technology*, 112 (1990) 456-464.
- [2] Wang, C.H., Brown, M.W., A path-independent parameter for fatigue under proportional and non-proportional loading, *Fatigue & Fracture of Engineering Materials & Structures*, 16 (1993) 1285-1297.
- [3] Itoh, T., Nakata, T., Sakane, M., Ohnami, M., Nonproportional low cycle fatigue of 6061 aluminum alloy under 14 strain paths, *European Structural Integrity Society*, 25 (1999) 41-54.
- [4] Socie, D.F., Marquis, G.B., *Multiaxial Fatigue*, Society of Automotive Engineers International, (2000).
- [5] Sakane, M., Itoh, T., Kida, S., Ohnami, M., Socie, D.F., Dislocation structure and non-proportional hardening of type 304 stainless steel, *European Structural Integrity Society*, 25 (1999) 130-144.
- [6] Itoh, T., Fukumoto, K., Hagi, H., Itoh, A., Saitoh, D., Low cycle fatigue damage of Mod.9Cr-1Mo steel under non-proportional multiaxial loading, *Procedia Engineering*, 55 (2013) 457-462.
- [7] Manson, S.S., A complex subject: some simple approximations, *Experimental mechanics*, 5 (1965) 193-226.
- [8] Itoh, T., Sakane, M., Ohnami, M., Socie, D.F., Nonproportional low cycle fatigue criterion for type 304 stainless steel, *Journal of Engineering Materials and Technology*, 117 (1995) 285-292.
- [9] Itoh, T., A model for evaluation of low cycle fatigue lives under nonproportional straining, *Journal of the Society of Materials Science*, 50 (2001) 1317-1322.
- [10] Itoh, T., Sakane, M., Hata, T., Hamada, N., A design procedure for assessing low cycle fatigue life under proportional and non-proportional loading, *International Journal of Fatigue*, 28 (2006) 459-466.
- [11] Itoh, T., Sakane, M., Shimizu, Y., Definition of stress and strain ranges for multiaxial fatigue life evaluation under non-proportional loading, *Journal of the Society of Materials Science*, 62 (2013) 117-124.
- [12] Itoh, T., Sakane, M., Ohsuga, K., Multiaxial low cycle fatigue life under non-proportional loading, *International Journal of Pressure Vessels and Piping*, 110 (2013) 50-56.
- [13] Itoh, T., Sakane, M., Morishita, T., Evaluation and visualization of multiaxial stress and strain states under non-proportional loading, *Frattura ed Integrità Strutturale*, 33 (2015) 289-301.
- [14] Coffin, L.F., *Mechanical Behavior of Materials*, 2 (1972) 516.